Control of the electronic properties of CdSe submonolayer superlattices via vertical correlation of quantum dots

I. L. Krestnikov,* M. Straßburg,† M. Caesar, A. Hoffmann, U. W. Pohl, and D. Bimberg
Institut für Festkörperphysik, Technische Universität Berlin, Hardenbergstrasse 36, 10623 Berlin, Germany

N. N. Ledentsov,‡ P. S. Kop'ev, and Zh. I. Alferov
A. F. Ioffe Physico-Technical Institute, Politechnicheskaya 26, St. Petersburg 194021, Russia

D. Litvinov, A. Rosenauer, and D. Gerthsen
Laboratorium für Elektronenmikroskopie der Universität Karlsruhe, Kaiserstrasse 12, Postfach 6980, 76128 Karlsruhe, Germany
(Received 5 August 1998)

Structural and optical properties of submonolayer CdSe/ZnSe superlattices grown with varying thickness of the ZnSe spacer layer are studied. High-resolution electron microscopy images demonstrate that submonolayer CdSe depositions result in two-dimensional nanoscale CdSe islands which are anticorrelated for spacer layer thicknesses exceeding 3 nm, while predominantly vertically correlated growth occurs for thinner spacers, in agreement with most recent theoretical predictions. Vertical ordering of the CdSe islands leads to two lines in photoluminescence (PL) and optical reflectance spectra originating from excitons localized at vertically coupled and uncoupled CdSe quantum islands, respectively. In edge PL, these lines exhibit different polarizations: predominantly TM and predominantly TE for coupled and uncoupled states, respectively. Stimulated emission in edge geometry and resonant waveguiding effects are observed for both states. The TE and TM components of the stimulated emission of the same state show an energy splitting. At the highest excitation densities we observe saturation of the stimulated emission in the edge geometry, and the development of a peak in surface emission that is strongly increasing with excitation intensity. This peak is attributed to stimulated emission in surface geometry, which is made possible by the ultrahigh material gain in quantum dots and the self-adjustment of the gain spectrum and the cavity mode. [S0163-1829(99)02024-X]

I. INTRODUCTION

Semiconductor heterostructures of reduced dimensionality like quantum wires (QW's),[1–6] and, particularly, quantum dots (QD's) have recently attracted much attention.[7–10] The most promising way to fabricate QW's and QD's is based on self-organized growth phenomena at crystal surfaces[11–14] or in the bulk, such as periodic surface faceting,[15–17] growth on faceted surfaces,[18–20] spontaneous phase separation of alloys,[21] and formation of two-dimensional[22–25] (2D) and three-dimensional[7,26,27] (3D) islands in heteroeptaxial growth. In order to display true 3D confinement effects the size of nanostructures must exceed a critical value to show confined states. On the other hand the structures must be small enough to ensure a sufficiently large energy separation of the charge-carrier sublevels to avoid thermal population of too many substates.[28] In wide-gap II–VI materials, a small size of the islands is indispensable to obtain 3D confinement due to the large electron and hole masses. The possibilities to control the electronic states and optical properties of nanoobjects by self-organization phenomena is usually, however, restricted due to a limited variation of geometrical size, shape, and degree of homogeneity. We propose an approach to overcome these limitations by using the possibility of anticorrelated or correlated growth of 2D islands.

Submonolayer (SML) insertions like CdSe in ZnSe are known to form dense and ordered arrays of nanoscale two-dimensional islands,[29] where two-dimensional islands are considered as objects with a high width/height ratio. Formation of ordered 2D surface structures (''parquet'' structures) caused by the coexistence of two phases on the surface, was first considered in Ref. 30. Marchenko[31] showed that two-dimensional islands (or, e.g., domains of identical surface reconstruction), differing in the value of intrinsic surface stress from adjacent areas, always exhibit partial relaxation of this surface stress at the domain boundaries. The formation of boundaries becomes energetically beneficial. The total energy per unit surface for an array of stripes on the surface can be written as[31]

$$E_{\mathrm{SURF}} = -\frac{\alpha}{L}\ln(\beta L) + \frac{\gamma}{L}, \tag{1}$$

where α, β, and γ are coefficients accounting for the difference in intrinsic surface stress between two phases and the role of the short-range potential due to additional dangling bonds formed at the island edges. The equilibrium size of the island (L_0) is determined by the minimum of Eq. (1) which exists at *any* finite positive values of coefficients α, β, and γ. In contrast, for homoepitaxial submonolayer deposition $\alpha = 0$, and the minimum energy corresponds to an infinite island size, which means the continuous ripening of 2D islands. Formation of ordered islands using strained submonolayer depositions has been demonstrated in a number of papers[22,23,24,29] for III–V and II–VI material systems. In our case the islands are strained by 7% lattice mismatch between CdSe and ZnSe. For strained covered 2D islands, partial relaxation of the elastic strain is possible near the island edges

at the expense of some strain in the host material. Thus there exist two sources of elastic deformation of the host material, and the situation is different from the case of 3D islands where the strain around an island gradually decreases with respect to its center. This more complex character of the strain distribution around 2D islands makes it possible that the islands in the subsequent layer on top of covered strained islands may arrange in two different ways: correlated (the islands in the subsequent layer are placed directly above the islands in the lower layer) or anticorrelated (the islands in the subsequent layer are placed *between* islands in the lower layer) growth.[29,32,33] We note that for 3D islands, the maximum distortion of the lattice constant that favors nucleation of the island in the subsequent layer always occurs on top of the underlying 3D islands. Shchukin *et al.*[13] showed that the possibility of vertical correlation or anticorrelation depends on both the elastic properties of the materials used and the ratio between the in-plane and vertical separation of islands. Transition from anticorrelated to correlated growth has been predicted for spacer layer thicknesses sufficiently small with respect to the lateral period.

In this work we investigate CdSe/ZnSe SML superlattices (SL's) with different ZnSe spacer layer thicknesses between CdSe sheets. For particular geometries of the structure we realize ordered arrays of two-dimensional islands grown either in a vertically correlated or anticorrelated way. For a narrow range of the spacer layer thicknesses a mixed situation occurs. Vertically coupled quantum islands demonstrate electronic properties which can be tuned by selecting the particular geometry of the structure.

II. EXPERIMENTAL DETAILS

A. Sample growth

The structures studied in this work are grown on n^+ GaAs(100) substrates using molecular beam epitaxy at a substrate temperature of 280 °C,[34,35] and were partially described elsewhere.[29] All structures consist of 360-nm ZnS_xSe_{1-x} buffer and 60-nm ZnS_xSe_{1-x} cap layers lattice matched to the GaAs substrate. Between these layers a CdSe/ZnSe SML SL is inserted. ZnSe barriers separate the sheets of CdSe SML insertions, and have thicknesses of 15, 30, 50, and 80 Å. The average thickness of a single CdSe insertion is about 0.7 ML, as evaluated by the DALI procedure. The total thickness of the SML SL region is 60 nm for structures with 30-, 50-, and 80-Å barriers, and 30 nm for the structure with 15-Å barriers. Consequently, the numbers of SL periods is different (20, 20, 12, and 8 for 15-, 30-, 50-, and 80-Å barriers, respectively). The thickness of the buffer layer corresponds to only a few photon wavelengths in the crystal. For this geometry, according to previous calculations,[36] the optical confinement of the light wave due to the *average* refractive index change between the active SML SL and the passive $ZnS_{0.06}Se_{0.94}$ cladding layers is negligible, and the emitted light should be effectively absorbed by the GaAs substrate, while the *in-plane* propagation is hardly possible.

B. Optical and structural characterization

The investigated II–VI SML SL's were characterized using photoluminescence (PL), optical reflection (OR), and photoluminescence excitation (PLE) spectroscopy. Gain studies have been performed in the edge geometry. The continuous-wave low excitation density PL measurements are carried out using a He-Cd laser with an excitation density of 3 W/cm^2 at 325 nm. To obtain OR data, the white light of a halogen lamp is used. The PL and OR spectra are analyzed using an 0.85-m Czerny-Turner double monochromator with a spectral resolution much better than 0.1 nm. The gain spectra are evaluated using the variable-stripe-length method.[37] For studies at high excitation densities a pulsed dye laser pumped by an excimer laser is used. The pulse duration is 20 ns at a rate of 50 Hz, providing maximum pulse energies of 400 mJ at 440 nm. The same laser system was used for PLE measurements. The samples are mounted in a helium flow cryostat providing fixed temperatures between 4 and 300 K.

Cross-section high-resolution transmission electron microscopy (HRTEM) is performed along the ⟨110⟩ direction using a PHILIPS CM 200 FEG/ST electron microscope with a Scherzer resolution of 0.24 nm. To reveal the distribution of the strained cadmium selenide insertions, digitized HRTEM images are processed by the evaluation program DALI (Ref. 38) that allows the determination of *local* lattice parameters (LLP's).

III. EXPERIMENTAL RESULTS AND DISCUSSION

A. Structural characterization

To investigate the structural properties of the samples we perform HRTEM measurements. A DALI processing of the lattice images is necessary to reveal the shape and size of quantum islands, as reported previously.[29] In Fig. 1 we show a color-coded map of the local lattice parameter in the growth direction ($a_\perp$) for the structures with 30-Å (a) and 15-Å (b) spacer layer thicknesses. The local lattice parameters are measured for each projected unit cell with the dimensions of $a_{001} \times a_{110}$. A reference lattice parameter is determined by which die LLP's are normalized. The reference lattice parameter for Fig. 1(a) was chosen to be the ZnS_xSe_{1-x} lattice constant resulting in LLP's between 1 and 1.07. An averaged lattice parameter was determined from the whole image [Fig. 1(b)]. Therefore, normalized LLP's smaller than 1 are observed in the ZnSe spacers. The shift in the color from blue to red corresponds to an increase of the lattice parameter in the vertical direction $a_\perp$. Thus the green, yellow, and red areas indicate (Cd, Zn)Se layers with larger LLP and, consequently, with larger Cd content, due to the larger bulk lattice parameter of CdSe (6.081 Å) with respect to that of the ZnSe (5.6697 Å). One can see that the CdSe insertions demonstrate different behaviors for these two cases. The areas with increased Cd content have lateral sizes of about ~40–50 Å for 30-Å spacers and of ~25–30 Å for 15-Å spacers. It should be noted that the measured Cd composition of the islands may be reduced due to the averaging effect along the thickness of the foil which ranges between 5 and 20 nm, and may therefore exceed the lateral island size. The estimated height of the Cd-rich insertions is about 2 and 4 ML. A broadening of the Cd distribution along the growth direction may be induced by steps along the electron beam or by the segregation of cadmium.

Formation of nanoscale islands by submonolayer depositions has already been demonstrated in this material

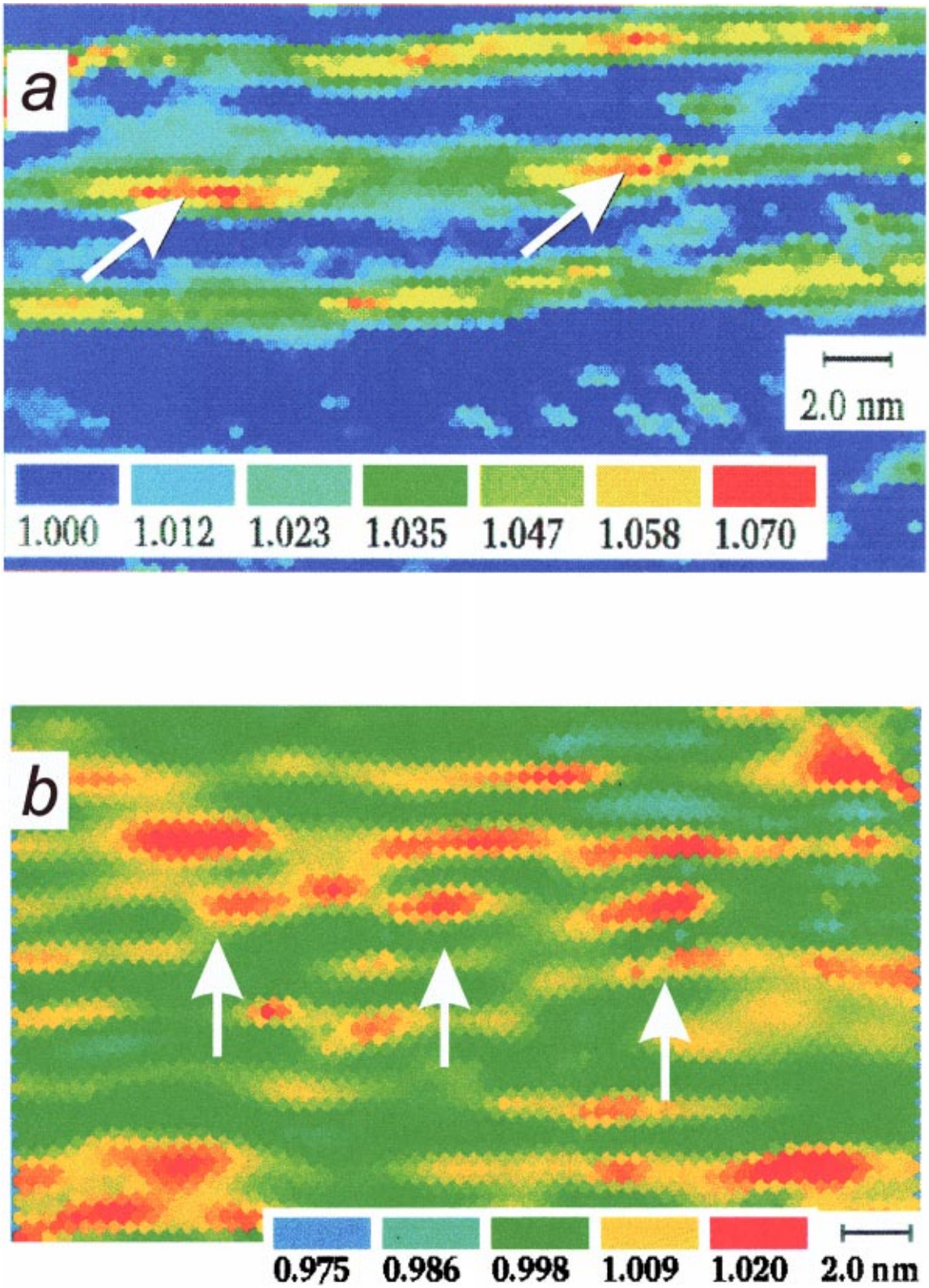

FIG. 1. (Color) Local lattice parameter map for stacked CdSe submonolayer structures with 30- and 15-Å ZnSe spacers. (a) is normalized to the ZnSe LLP, while in (b) an average LLP was obtained and used for normalization.

system.[25,29] The remarkable change in the lateral arrangement of islands with decrease of the spacer layer thickness is reported here. A close inspection of Fig. 1(a) reveals that the islands in the upper sheets which are separated by 30-Å spacers tend to nucleate at positions between the islands of the previous sheet (anticorrelated growth) while a vertical arrangement of islands over a period of 2–5 layers is locally observed for the structure with the 15-Å spacers [Fig. 1(b)]. As recently calculated by Shchukin *et al.*,[13] the character of vertical ordering of two-dimensional islands depends crucially on the relative thickness of the spacer layer with respect to the lateral period of the structures. For small spacers,

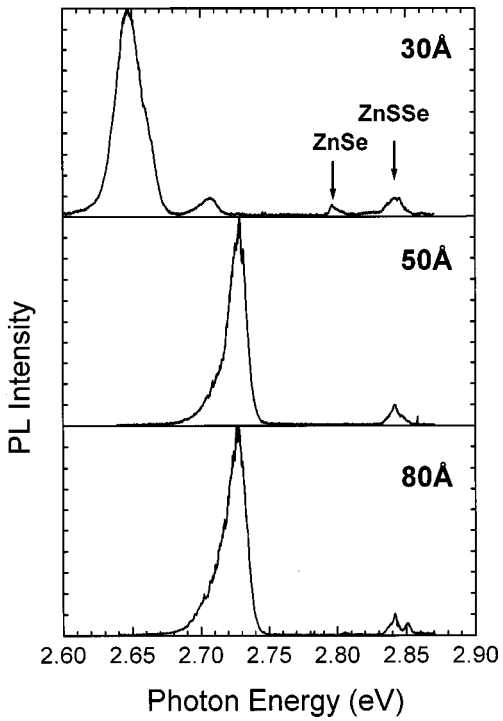

FIG. 2. Photoluminescence (PL) spectra of samples with different thicknesses of the ZnSe spacer layers [the registration temperature (T_{reg}) is 7 K, the excitation density (P_{exe}) 5 kW/cm^2, and the energy of the exciting photon (E_{exe}) is 2.88 eV].

a transition from anticorrelated to correlated growth occurs if the spacer layer thickness is decreased to about one-third of the lateral period. Since the lateral period for 30-Å spacer structures [Fig. 1(a)] can be roughly estimated to be 10 nm; the transition is expected to occur at a spacer layer thickness of 3 nm. This is in very good agreement with our experimental data. We note, however, that we do not see continuous vertical chains of QD's through the entire structure, being typical for vertically coupled three-dimensional quantum dots.[10,39] Three to four periods of stacking predominantly occur. Moreover, some of the chains are tilted. The average lateral size of the islands is smaller than in the case of anticorrelated growth. We attribute these effects to the high complexity of the system. Theoretical calculations of vertical ordering of islands in Ref. 13 do not consider the influences of the strain fields produced by underlying islands on the island lateral size in the upper row, and refer only to the relative arrangement of islands. The effect of the strain on the island size can be important exactly in the case of ultrathin spacers. Nevertheless, the stacking of three periods already has a strong impact on the PL properties, as was shown for similar structures grown by metal-organic vapor phase epitaxy.[40]

B. Electronic properties

The properties of electronic states in quantum islands are studied by optical investigations. PL spectra of structures having different spacer layer thicknesses are shown in Fig. 2. For large spacer layer thickness only one line appears. The transition energies correspond to heavy-hole-like excitons which are localized at two-dimensional nanoscale islands with lateral extensions comparable to the exciton diameter.

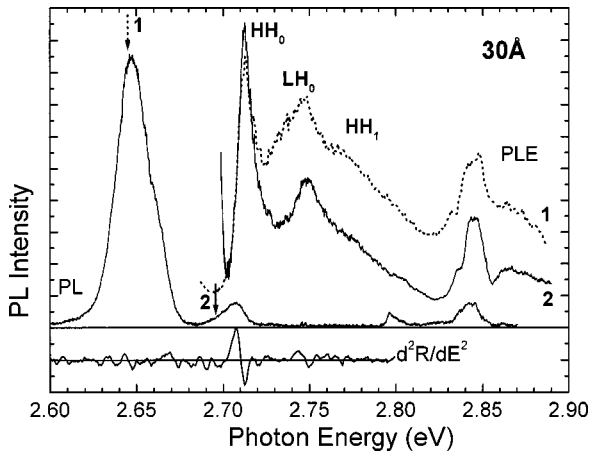

FIG. 3. PD and PL excitation (PLE) spectra and second derivative of the optical reflectance spectrum for the structure with 30-Å spacers. Detection energies for the PLE spectra are shown by arrows. (T_{reg}=7 K, and P_{exe}=5 kW/cm^2).

On the other hand, at a spacer layer thickness of 30 Å, a second lower-energy luminescence line evolves. The arrangement of islands in a vertical correlation results in an efficient coupling of electronic states between vertically neighboring islands, because the main part of the wave function is extended into the barrier. The appearance of the low-energy line can thus be assigned to such chains of coupled quantum dots. The low-energy shift of the luminescence is similar to the case of vertically coupled QD's, as demonstrated first for 3D InAs-GaAs QD's.[10,41] A further decrease of the spacer thickness results in an increased intensity of the PL due to enhanced coupling of QD's, and in a complete suppression of the luminescence from uncoupled islands.

The optical spectra of the SML SL with 30-Å spacer shown in Fig. 3 give further information about the electronic states. The main luminescence line originates from coupled QD's, while the main feature in the OR spectrum appears at 2.71 eV, and corresponds to uncoupled states. This can be explained by the fact that, even if the density of uncoupled QD's is still larger than that of the coupled QD's, an efficient hopping and tunneling of carriers from higher-lying uncoupled states results in predominant population of the coupled states. The higher density of uncoupled QD's is confirmed by the fact that the PLE spectra of both peaks demonstrate essentially the same shape with main resonance, corresponding to heavy- and light-hole like excitons in uncoupled QD's.

We note that in the PLE spectra of uncoupled states one can clearly see a ground state and two excited states. As shown previously by circularly and linearly polarized PL and PLE measurements,[36] the lowest, first, and second excited states have heavy-, light-, and heavy-hole-like characters, respectively. The appearance of the second heavy-hole-like excited state HH_1 can be explained by only lateral quantization, because a second heavy-hole-like subband is not possible in the case of ultrathin CdSe quantum wells. Similar spectra are observed for all structures with anticorrelated or noncorrelated growth, i.e., samples with 30-, 50-, and 80-Å spacers.

The edge emission of anticorrelated or uncorrelated SML QD's is predominantly TE polarized,[36] because the 2D shape of the islands results in much stronger heavy-hole k quanti-

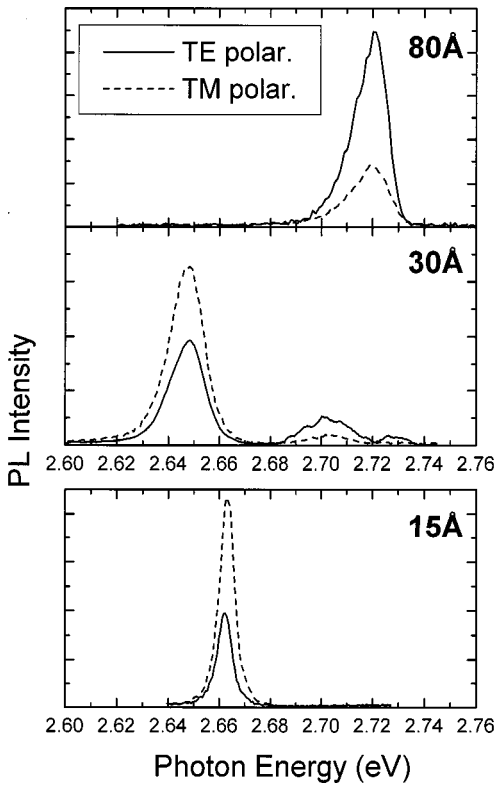

FIG. 4. Linearly polarized spectra of edge emission for structures with 80-, 30-, and 15-Å spacers. ($T=7$ K, $P_{exe}=3$ W/cm^2, and $E_{exe}=3.81$ eV). The PL energies of the low-energy transition of the 15- and 30-Å spacer samples differ due to different lateral island sizes.

zation in the growth direction, as compared to the lateral direction. Thus, the heavy-hole-like exciton emission is predominantly TE-polarized (50–60 %), even if lateral quantization also enables a TM-like emission. This depolarization is not possible in a quantum well, where the heavy-hole exciton emission is completely TE polarized. We note also that for spherical or cubic QD's, no predominant polarization of the exciton luminescence should be observed. Since vertical coupling of islands results in an extension of the heavy-hole wave function in the growth direction, the *k*-quantization effect is reduced. Therefore, a different polarization of the low-energy line is expected.

Polarized PL spectra of structures with 80-, 30-, and 15-Å spacers, measured in edge geometry, are shown in Fig. 4. We note that the different PL energies of the low-energy transitions are caused by the different lateral island sizes (see Fig. 1), probably due to the influence of the strain field on the lateral island size. The smaller lateral size for the 15-Å spacer sample leads to a stronger in-plane quantization in this sample. In the structure with 30-Å spacers, the polarization of the low-energy line which is related to coupled QD's is reversed with respect to the polarization of anticorrelated islands. The high-energy line shows the same polarization as the uncoupled islands of the sample with 80-Å spacers, so confirming an uncorrelated arrangement. Furthermore, the low-energy luminescence exhibits a polarization like that on the sample with 15-Å spacers, indicating a spatial correlation. This marked result clearly points to a delocalization of the heavy-hole-like QD exciton state along the growth axis, and manifests a formation of coupled QD states. The effects clearly demonstrate a way to engineer QD exciton wave functions using the correlated QD growth, and provide unique possibilities for polarization control of edge-emitting lasers. We note here that the degree of polarization of the edge emission is uniform within the shape of the corresponding line.

C. Gain spectrum of uncoupled islands

The principal advantage of SML SL's composed of dense arrays of two-dimensional QD's is the possibility to realize an intrinsic resonant waveguiding effect (excitonic waveguide) even without thick cladding layers having a lower refractive index.[25,42–44] The effect is based on a resonant enhancement of the refractive index in the vicinity of the exciton resonance in accordance with Kramers-Kronig equations. Since the studied structures are grown with thin buffer layers directly on the strongly absorbing GaAs substrate, the resonant modulation of the refractive index must be remarkably strong to provide resonant waveguiding. This is possible because of the ultrahigh material gain in QD's and their remarkably high density for stacked SML depositions. Another strict requirement to enable excitonic waveguiding is the lifting of the *in-plane k*-selection rule, which prohibits zero-phonon emission of excitons with finite kinetic energy that dominate in bulk and quantum-well structures at high temperatures or excitation densities. In the latter structures, phonon-assisted gain is possible,[37] but it occurs out of the energy range of efficient resonant waveguiding. On the other hand, in-plane *k*-selection rules are not appropriate in QD's, and zero-phonon gain resonant to the resonant waveguiding region is possible without using of thick cladding layers with low refractive index.

Therefore, we are able to realize gain at high excitation density and observe stimulated emission in all the structures under investigation. Gain spectra with both TE and TM emission are observed for the structure with 50-Å spacers, where only the emission from uncoupled states appears. Stimulated emission demonstrates a stronger degree of TE polarization, as can be expected in view of the stronger amplification of the TE mode. Surprisingly, we observed an appearance of the TM mode peak exactly at the energy which corresponds to the heavy-hole-like exciton state revealed in the PLE and OR spectra (Fig. 5). The observation of the polarization reversal within the contour of the same stimulated emission peak is very unusual for any kinds of laser structures studied up to now. Probable explanation is the development of the collective photonic states in QD ensembles,[45] resulting from electromagnetic interaction of QD's. This effect is predicted to cause a splitting of the gain peak into TE and TM components in arrays of QD's having an anisotropic QD shape and (or) relative arrangement.

A comparison of the surface PL at high excitation densities and stimulated emission recorded from the edge of the structure is shown in Fig. 6. The transition energies from the QD ground state revealed in the OR spectra of the structures are shown by solid segments. The features observed in the surface emission of the 80- and 50-Å spacer structures will be discussed below. The stimulated emission originates from uncoupled QD structures with larger spacer layer thicknesses. Emission from coupled states dominates only in case

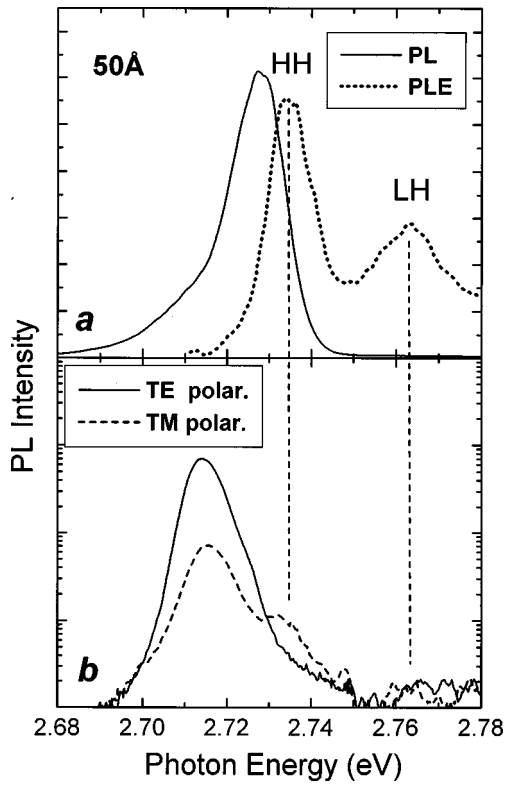

FIG. 5. PL and PLE spectra (a) and linearly polarized spectra of stimulated emission (b) for the structure with 50-Å spacers ($T_{reg}=7$ K, $P_{exe}=1$ MW/cm^2, and $E_{exe}=2.88$ eV).

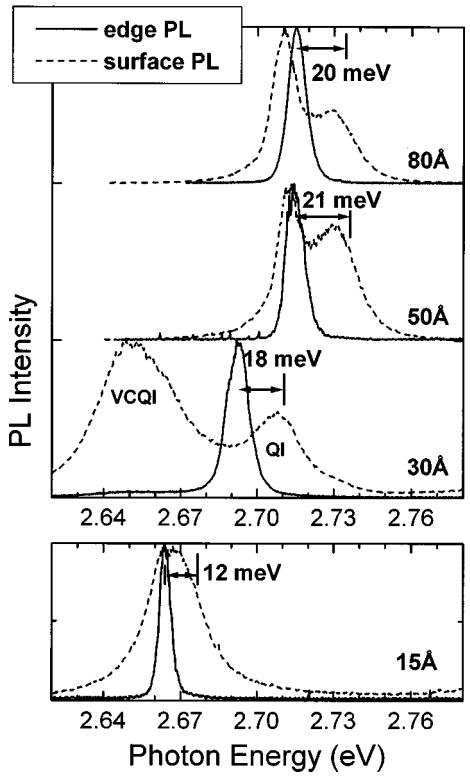

FIG. 6. Edge and surface PL of structures with different spacer layer thickness ($T_{reg}=7$ K, $P_{exe}=1$ MW/cm^2, and $E_{exe}=2.88$ eV). The PL energies of the low-energy transition of the 15- and 30-Å spacer samples differ due to different lateral island sizes.

of the 15-Å spacers, where the density of the coupled states is high. The zero-phonon nature of the QD emission is confirmed by the energy positions of the stimulated emission and the gain maximum. The redshift of the stimulated emission is distinctly smaller than the LO-phonon energy, proving the zero-phonon gain mechanism for all the structures. The energy position of the gain maximum does not shift with the excitation density, manifesting an exciton gain mechanism in the exciton waveguiding region.

Gain spectra of the structure with uncoupled QD's at excitation densities well above threshold of stimulated emission are depicted in Fig. 7. One can clearly see that the absorption peak which appears in the region of excitonic waveguiding remains even at excitation densities as high as two orders of magnitude above the threshold. Thus there still exists a spectral range of strong excitonic absorption providing an increased refractive index on its low-energy side, and, consequently, an efficient exciton-induced waveguiding. At the highest excitation densities, however, the situation starts to change. The gain saturates with increasing excitation density, and even a decrease in gain is observed. The effect is accompanied by a saturation of the edge emission. This effect can be explained by a partial saturation of the excitonic waveguiding effect. Since stimulated emission can occur only in the narrow spectral energy range due to exciton-induced refractive index enhancement, not each QD can contribute to the gain. The number of QD's having a proper transition energy is finite, and, after filling of these QD's, gain saturates. At very high excitation levels when all the QD's are filled, there is no excitonic absorption and, conse-

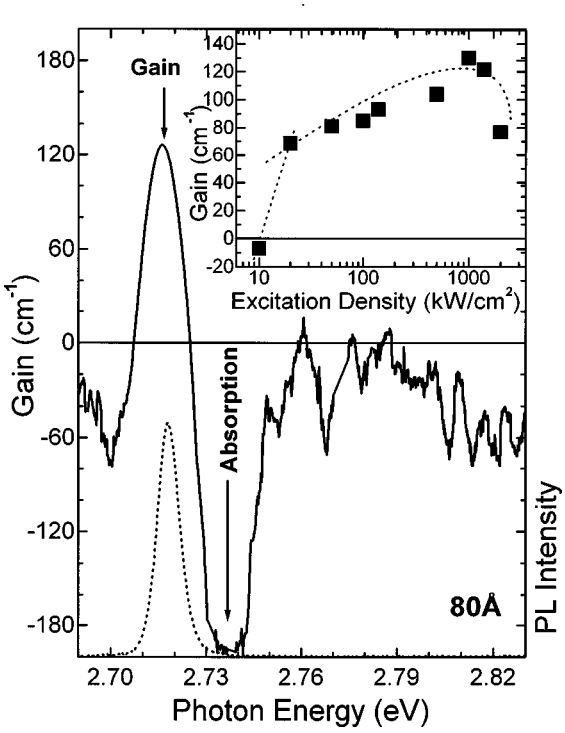

FIG. 7. Gain (solid line) and stimulated emission (dotted line) spectra for the structure with 80-Å spacers ($T_{reg}=7$ K, $P_{exe}=1$ MW/cm^2, and $E_{exe}=2.88$ eV). The inset shows the dependence of the maximum gain on excitation density.

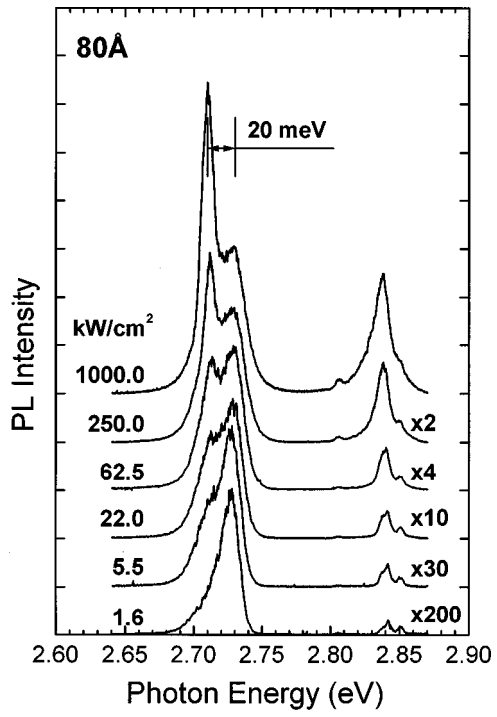

FIG. 8. Surface PL spectra for the structure with 80-Å spacers at different excitation densities ($T_{reg}=7$ K and $E_{exe}=2.88$ eV).

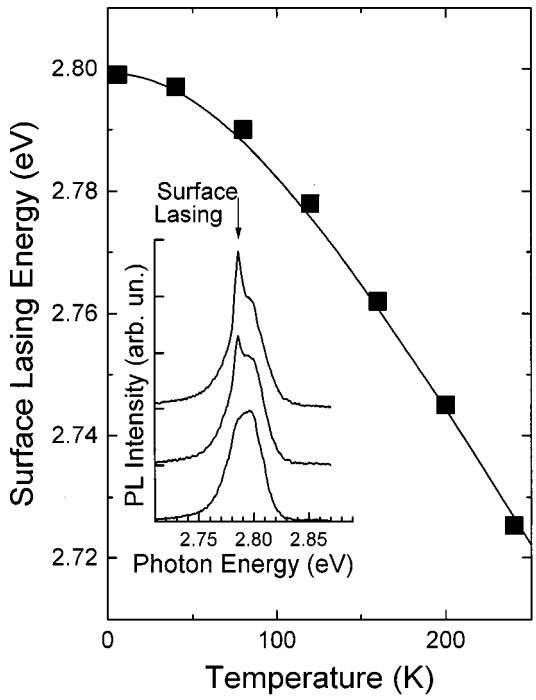

FIG. 9. Temperature dependence of the surface lasing energy for the structure with 30-Å spacers and $ZnMgS_xSe_{1-x}$ barriers. PL spectra below (a) and above (b) thresholds are shown in the inset.

quently, also non-exciton-induced waveguiding on the low-energy side of the excitonic resonance. This results in a decrease of the gain.

Simultaneously with the saturation of the edge emission a new line appears in the surface PL spectra shifted by about 20 meV to the low-energy side from the exciton resonance energy (Fig. 8; see also Fig. 6). The superlinear growth of the intensity of this line occurs at already very high excitation densities. Both effects taken together hint at the observation of stimulated emission in surface geometry. This process is possible if the gain in the structure overcomes losses, which are external losses in this case in view of the small cavity thickness. These losses can be roughly evaluated as

$$\alpha_{\text{ext}}=\frac{1}{2L}\ln\left(\frac{1}{R_1R_2}\right), \tag{2}$$

where R_1 and R_2 are the reflectivity of the surface and the GaAs-ZnSe interface, respectively. Equation (2) gives an estimate of the losses of about $4\times10^4\,\text{cm}^{-1}$. Assuming that the active gain region takes only 13% of the total vertical cavity length, the modal gain should exceed $3\times10^5\,\text{cm}^{-1}$. This value is huge, but can be expected for dense arrays of small QD's having relatively small inhomogeneous broadening.[46–48] In a similar structure it was shown by Aliev *et al.*[49] that the optical density of CdSe SML SL is about 0.5. Taking into account a SL thickness of 600 Å, the absorption coefficient can be estimated to be $1\times10^5\,\text{cm}^{-1}$. Thus the gain can attain this value or even exceed it up to a factor of 2 due to the biexciton contribution. In this case, the modulation of refractive index due to the Kramers-Kronig equations becomes comparable with the refractive index in the surrounding matrix. This can significantly increase the reflectivity of the mirrors. Another point is the fitting of the lasing energy to the cavity mode, which must depend on the cavity thickness. For a variable refractive index within the contour of the gain spectrum, however, a self-adjustment effect takes place, and the standing-wave condition is automatically fulfilled,[50] if the difference of the gain wavelength and the cavity mode is not too large.

The proof of the self-adjustment effect is the shift of the lasing mode with the gain spectrum. This can be realized by changing the temperature. To monitor the behavior in a wide spectral range we used a structure with CdSe SML insertions in a $ZnMgS_xSe_{1-x}$ matrix, providing better localization of carriers and permitting lasing up to room temperature.[51] In Fig. 9 we show the temperature dependence of the surface lasing energy. PL spectra of the structure below and above threshold are shown in the inset. As-it-follows from Fig. 9, the lasing energy follows the matrix band-gap temperature dependence which is much stronger than the usual temperature dependence of the cavity mode. The latter is weak because it originates from a change of the refractive index of the matrix material. Thus the self-adjustment effect seems to be the most probable explanation of the stimulated emission in surface geometry.

IV. CONCLUSIONS

To conclude, we demonstrated that by proper selection of the structure geometry by using submonolayer depositions one can tune the vertical arrangement of submonolayer islands and consequently the electronic spectrum of quantum

dots. We demonstrated that the polarization of the luminescence in edge geometry is opposite for coupled and uncoupled two-dimensional quantum dots. We observed resonant waveguiding and stimulated emission in edge geometry for both types of quantum dots. At very high excitation densities we found strong evidence for stimulated emission in surface geometry in structures without Bragg reflectors, and attributed the effect to ultrahigh material gain in submonolayer quantum dots and a self-adjustment effect of the gain spectrum and the cavity mode.

ACKNOWLEDGMENTS

We are grateful to Dr. S. V. Ivanov and Dr. S. V. Sorokin for the growth of the samples. This work was supported by the Russian Foundation on Basic Research (Grants No. 97-02-18138 and 97-02-18269a), the Program of Ministry of Science of the Russian Federation ''Physics of Solid-States Nanostructures'' (Projects No. 97-2014 and 97-1035), and the Deutsche Forschungsgemeinschaft (DFG). I.L.K. and N.N.L. are grateful to the DFG and to the Alexander von Humboldt Foundation, respectively.

*On leave from Ioffe Institute, St. Petersburg, Russia.

†Author to whom correspondence should be addressed. FAX: 49-30-314-22064. Electronic address: marburg@mail.physik.tu-berlin.de

‡Also at Institut für Festkörperphysik, Technische Universität, Berlin, Germany.

[1] J. M. Worlock, F. M. Peeters, H. M. Cox, and P. C. Morais, Phys. Rev. B **44**, 8923 (1991).

[2] R. Nötzel, N. N. Ledentsov, L. Däweritz, K. Ploog, and M. Hohenstein, Phys. Rev. B **45**, 3507 (1992).

[3] M. S. Miller, H. Weman, C. E. Pryor, M. Krishnamurthy, P. M. Petroff, H. Kroemer, and J. L. Merz, Phys. Rev. B **68**, 3464 (1992).

[4] H. Akiyama, T. Someya, and H. Sakaki, Phys. Rev. B **53**, R16160 (1996).

[5] F. Liu, J. Tersoff, and M. G. Lagally, Phys. Rev. Lett. **80**, 1268 (1998).

[6] G. Biasiol, E. Kapon, Y. Ducommun, and A. Gustafsson, Phys. Rev. B **57**, R9416 (1998).

[7] L. Goldstein, F. Glass, J. Y. Marzin, M. N. Charasse, and G. Le. Roux, Appl. Phys. Lett. **47**, 1099 (1985).

[8] P. M. Petroff and S. P. Den Baars, Superlatt. Microstruct. **15**, 15 (1994).

[9] M. Moison, F. Houzay, F. Barthe, L. Leprince, E. Andre, and O. Vatel, Appl. Phys. Lett. **64**, 196 (1994).

[10] N. N. Ledentsov, M. Grundmann, N. Kirstaedter, J. Christen, R. Heitz, J. Böhrer, F. Heinrichsdorff, D. Bimberg, S. S. Ruvimov, P. Werner, U. Richter, U. Gösele, J. Heydenreich, V. M. Ustinov, A. Yu. Egorov, M. V. Maximov, P. S. Kop'ev, and Zh. I. Alferov, in *Proceedings of the ICPS*, edited by D. J. Lockwood (World Scientific, Singapore, 1995), Vol. 22, p. 1855.

[11] V. A. Shchukin, N. N. Ledentsov, P. S. Kop'ev, and D. Bimberg, Phys. Rev. Lett. **75**, 2968 (1995).

[12] V. A. Shchukin, N. N. Ledentsov, M. Grundmann, P. S. Kop'ev, and D. Bimberg, Surf. Sci. **352-354**, 117 (1996).

[13] V. A. Shchukin, D. Bimberg, V. G. Malyshkin, and N. N. Ledentsov, Phys. Rev. B **57**, 12 262 (1998).

[14] V. A. Shchukin and D. Bimberg, Rev. Mod. Phys. (to be published).

[15] R. J. Phaneuf and E. D. Williams, Phys. Rev. Lett. **58**, 2563 (1987).

[16] R. J. Phaneuf, E. D. Williams, and N. C. Bartlet, Phys. Rev. B **38**, 1984 (1988).

[17] E. D. Williams, R. J. Phaneuf, Jian Wei, N. C. Bartlet, and T. L. Einstain, Surf. Sci. **294**, 219 (1993).

[18] M. Kasu and N. Kobayashi, Appl. Phys. Lett. **62**, 1262 (1993).

[19] N. N. Ledentsov, G. M. Gurianov, G. E. Tsyrlin, V. N. Petrov, Yu. B. Samsonenko, A. O. Golubok, and S. Ya. Tipisev, Fiz. Tekh. Poluprovodn. **28**, 903 (1994) [Semiconductors **28**, 526 (1994)].

[20] R. Nötzel, N. N. Ledentsov, L. Däweritz, M. Hohenstein, and K. Ploog, Phys. Rev. Lett. **62**, 3812 (1991).

[21] J. W. Cahn, Trans. Metall. Soc. AIME **242**, 166 (1968).

[22] P. D. Wang, N. N. Ledentsov, C. M. Sotomayor Torres, P. S. Kop'ev, and V. M. Ustinov, Appl. Phys. Lett. **64**, 1526 (1994).

[23] P. D. Wang, N. N. Ledentsov, C. M. Sotomayor Torres, P. S. Kop'ev, and V. M. Ustinov, Appl. Phys. Lett. **66**, 112 (1995).

[24] V. Bressler-Hill, A. Lorke, S. Varma, P. M. Petroff, K. Pond, and W. H. Weinberg, Phys. Rev. B **50**, 8479 (1994).

[25] N. N. Ledentsov, I. L. Krestnikov, M. V. Maximov, S. V. Ivanov, S. V. Sorokin, P. S. Kop'ev, Zh. I. Alferov, D. Bimberg, and C. M. Sotomayor Torres, Appl. Phys. Lett. **70**, 2888 (1997).

[26] D. E. Eaglesham and M. Cerullo, Phys. Rev. Lett. **64**, 1943 (1990).

[27] J.-W. Mo, D. E. Savage, B. S. Swatzentruber, and M. G. Lagally, Phys. Rev. Lett. **65**, 1020 (1990).

[28] M. Grundmann, O. Stier, and D. Bimberg, Phys. Rev. B **52**, 11 969 (1995).

[29] M. Strassburg, V. Kutzer, U. W. Pohl, A. Hoffmann, I. Broser, N. N. Ledentsov, D. Bimberg, A. Rosenauer, U. Fischer, D. Gerthsen, I. L. Krestninov, M. V. Maximov, P. S. Kop'ev, and Zh. I. Alferov, Appl. Phys. Lett. **72**, 942 (1998).

[30] C. Herring, Phys. Rev. **82**, 87 (1951).

[31] V. I. Marchenko, Pis'ma Zh. Eksp. Teor. Fiz. **33**, 397 (1981) [JETP Lett. **33**, 381 (1981)].

[32] V. Calvo, P. Lefebvre, V. Allegre, A. Bellabchara, H. Mathieu, Q. X. Zhao, and N. Magnea, Phys. Rev. B **53**, R16164 (1996).

[33] P. Lefebvre, V. Calvo, N. Magnea, Th. Taliercio, J. Allegre, and H. Mathieu, Phys. Rev. B **56**, 3907 (1997).

[34] S. V. Ivanov, S. V. Sorokin, P. S. Kop'ev, J. R. Kim, H. D. Jung, and H. S. Park, J. Cryst. Growth **159**, 1 (1996).

[35] S. V. Ivanov, A. A. Toropov, T. V. Shubina, S. V. Sorokin, A. V. Lebedev, I. V. Sedova, P. S. Kop'ev, G. R. Pozina, J. P. Bergman, and B. Monemar, J. Appl. Phys. **83**, 3168 (1998).

[36] I. L. Krestnikov, M. V. Maximov, A. V. Sakharov, P. S. Kop'ev, Zh. I. Alferov, N. N. Ledentsov, D. Bimberg, and C. M. Sotomayor Torres, J. Cryst. Growth **184/185**, 545 (1998).

[37] C. Benoit a la Guillaume, J. M. Denber, and F. Salvan, Phys. Rev. **177**, 567 (1969).

[38] A. Rosenauer, S. Kaiser, T. Reisinger, J. Zweck, W. Gebhardt, and D. Gerthsen, Optik (Stuttgart) **102**, 63 (1996).

[39] N. N. Ledentsov, V. A. Schukin, M. Grundman, N. Kirstaedter, J. Bohrer, O. Schmidt, D. Bimberg, S. V. Zaitsev, V. M. Ustinov, A. E. Zhukov, P. S. Kop'ev, Zh. I. Alferov, O. A. Kosogov, S. S. Ruvimov, P. Werner, U. Gosele, and J. Heydereich, Phys. Rev. B **54**, 8743 (1996).

[40] U. W. Pohl, R. Engelhardt, V. Türck, and D. Bimberg, J. Cryst. Growth **195**, 569 (1998).

[41] Zh. I. Alferov, N. A. Bert, A. Yu. Egorov, A. E. Zhukov, P. S. Kop'ev, I. L. Krestnikov, N. N. Ledentsov, A. V. Lunev, M. V. Maximov, A. V. Sakharov, V. M. Ustinov, A. F. Tsatsul'nikov, Yu. M. Shernyakov, and D. Bimberg, Fiz. Tekh. Poluprovodn. **30**, 191 (1996) [Semiconductors **30**, 193 (1996)].

[42] I. L. Krestnikov, M. V. Maximov, N. N. Ledentsov, S. V. Ivanov, S. V. Sorokin, P. S. Kop'ev, and Zh. I. Alferov, in *Proceedings of the 23rd International Conference on the Physics of Semiconductors, Berlin, Germany, July 21–26, 1996*, edited by M. Scheffler and R. Zimmermann (World Scientific, Singapore, 1996), Vol. 4, p. 3178.

[43] N. N. Ledentsov, I. L. Krestnikov, M. V. Maximov, S. V. Ivanov, S. V. Sorokin, P. S. Kop'ev, Zh. I. Alferov, D. Bimberg, and C. M. Sotomayor Torres, Appl. Phys. Lett. **69**, 1343 (1996).

[44] I. L. Krestnikov, M. V. Maximov, S. V. Ivanov, N. N. Ledentsov, S. V. Sorokin, A. F. Tsatsul'nikov, O. G. Lublinskava, B. V. Volovik, P. S. Kop'ev, and C. M. Sotomayor Torres, Fiz. Tekh. Poluprovodn. **31**, 229 (1997) [Semiconductors **31**, 127 (1997)].

[45] G. Ya. Slepyan, S. A. Maksimenko, V. P. Kalosha, J. Herrmann, N. N. Ledentsov, I. L. Krestnikov, Zh. I. Alferov, and D. Bimberg, Phys. Rev. Lett. (to be published).

[46] M. Asada, A. Kameyama, and Y. Suematsu, IEEE J. Quantum Electron. **20**, 745 (1984).

[47] L. V. Asryan, R. A. Suris, Semicond. Sci. Technol. **11**, 554 (1996).

[48] M. Grundmann and D. Bimberg, Phys. Rev. B **55**, 9740 (1997).

[49] G. N. Aliev, A. D. Andreev, R. M. Datsiev, S. V. Ivanov, S. V. Sorokin, A. B. Kapustina, I. L. Krestnikov, M. E. Sasin, and R. P. Seisyan, J. Cryst. Growth **184/185**, 315 (1998).

[50] N. N. Ledentsov, V. M. Ustinov, Zh. I. Alferov, D. Bimberg, V. P. Kalosha, and J. A. Lott (unpublished).

[51] A. V. Sakharov, S. V. Ivanov, S. V. Sorokin, I. L. Krestnikov, B. V. Volovik, N. N. Ledentsov, and P. S. Kop'ev, Pis'ma Zh. Tekh. Fiz. **23**, 1997 (1997) [Tech. Phys. Lett. **23**, 305 (1997)].